THE AMERICAN SOCIETY OF MECHANICAL ENGINEERS
345 E. 47th St., New York, N.Y. 10017

97-GT-55

OFF-DESIGN FLOW ANALYSIS AND PERFORMANCE PREDICTION OF AXIAL TURBINES

Milan V. Petrovic
Faculty of Mechanical Engineering
University of Belgrade
27. Marta 80, 11000 Belgrade
Yugoslavia

Walter Riess
Institute for Turbomachinery
University of Hanover
Appelstr. 9, 30167 Hanover
Germany

ABSTRACT

Through-flow methods for calculations in axial flow turbines are limited by two facts: they cannot handle local flow reversal, and loss prediction at off-design operating conditions is not sufficiently accurate. An attempt to overcome these limitations is presented in this paper. The developed calculation method is based on the through-flow theory and the finite element solution procedure, but it also includes extensions and improvements. Consequently, the method may be used to predict the flow field and the turbine performance at the design load as well as for wide range of part loads. The code is able to calculate flow in axial turbines at subsonic and transonic conditions. The reliability of the method is verified by calculations for several gas and steam turbines. Results of flow calculation and performance prediction of 4-stage experimental air turbine and LP steam turbine are also presented herein. Low load operation with flow reversal in the hub region behind the last rotor blade row and loads, at which part of blading operates with power consumption, are especially analyzed. All numerical results are compared to the results of extensive experimental investigations. The correspondence, even for low loads, is very good.

NOMENCLATURE

a	throat width
b	tangential blockage factor
c	absolute velocity
d	tangential blade thickness
f	height of the camber line
H	stagnation enthalpy
h	static enthalpy, blade height
$\bar{h}$	relative blade height, fraction of span
I	rothalpy
K_a, K_ya	correcting factors (Eq. 14)
Ma	Mach number
$\dot{m}$	mass flow rate
n	rotational speed (rpm)
p	pressure
r	radial coordinate
s	entropy
t	temperature, pitch
u	peripheral velocity
w	relative velocity
y	wetness fraction
z	axial coordinate
β	flow angle (from tangential direction)
β_s	stagger angle
$\Delta\beta^*$	non-dimensional function of incidence angle $\Delta\beta$
γ	cascade coefficient
δ	deflection angle
ε	cascade pressure ratio
ζ	loss coefficient
η	efficiency
κ	ratio of specific heat
Π	pressure ratio
ρ	density
ψ	stream function

Subscripts

Cl	clearance	T	tip
H	hub	ts	total to static
in	inlet	u	circumferential component
out	outlet	z	axial component
P	profile	0	design conditions
r	radial component	1	inlet
S	secondary	2	outlet
s	isentropic		

Presented at the International Gas Turbine & Aeroengine Congress & Exhibition
Orlando, Florida — June 2–June 5, 1997

INTRODUCTION

In steam turbines, off-design conditions occur in several occasions, e. g. at start-up, shutdown, at overnight part load operation, etc. Regulated steam extraction upstream the LP part may result in continuous LP-operation at very low steam flow. At turbines for district-heating plants, minimizing mass flow rate through LP-part is attempted, because of the increasing heat needs at low atmospheric temperature. Gas turbines operation is frequently associated with significant changes in operating conditions. Considerable deviation of flow from the design conditions causes increase in flow losses and decrease in turbine efficiency. Flow phenomena, like flow separation, local reversal and operation with power consumption of a part of turbine blading, occur at very low loads.

During the design phase, the accurate flow calculation at nominal conditions enables parameter variation and optimization of turbine construction and, therefore, increase in turbine efficiency. Knowledge of the flow and turbine behavior over the wide range of operating conditions is of great importance, not only for performance optimization, but also for reliability improvement.

Through-flow calculation methods are widely used in turbomachinery design because of their speed and efficiency. Most through-flow calculation procedures are based on the general theory of Wu (1952). Smith (1966), Bosman and Marsh (1974), Hirsch and Warzee (1976), Denton (1978) and others have improved the theoretical model and developed different methods for solution. Nevertheless, the application of through-flow methods for flow calculations in axial flow gas and steam turbines at part and low loads is still connected with considerable limitations and uncertainty. Flow separation and reversal, which occur in the hub region behind the last rotor blade row at low load operation, cannot usually be handled, and correlations for calculation of loss coefficients at off-design conditions are not sufficiently accurate. Therefore, especially in industry, there exists significant interest in further improvement of through-flow methods for economical flow calculation of multistage turbines in design phase.

This paper presents the development of computational method for quick and accurate flow analysis and performance prediction of multistage gas and steam turbines over very wide range of operating conditions. The method is based on the through-flow theory and finite element procedure. It includes some extensions and improvements in form of new combination of loss and deviation correlations, losses radial distribution, spanwise mixing, new procedure for density calculation, and extension to encompass local reverse meridional flow. The results of calculations for 4-stage experimental air turbine of Institute for Turbomachinery, University of Hanover, and for one LP steam turbine is presented herein, as well as the comparison of numerical data with results of extensive experimental investigations.

FLOW PHENOMENA IN TURBINE OFF-DESIGN OPERATION

At part loads, the volume flow through the last blade rows is reduced . Considerable flow deviation from design conditions causes the increase of cascade incidence angles and profile losses, and, consequently, the decrease in turbine efficiency and stage capability in generating mechanical work. Under very low flow conditions, the velocity diagrams might change so much that part of blading, beginning at the last stage, starts to work with energy consumption, i. e., rotating blades transmit energy into the flow by local ventilation. At far off-design operation, flow separation and flow reversal occur in the hub region behind the last rotor blade row. In case of further reduction of volume flow, the separation extends to the turbine blading and vortices are formed in axial gaps between the blade rows. These phenomena which appear at part loads and low loads may disturb reliable turbine operation and lead to damages.

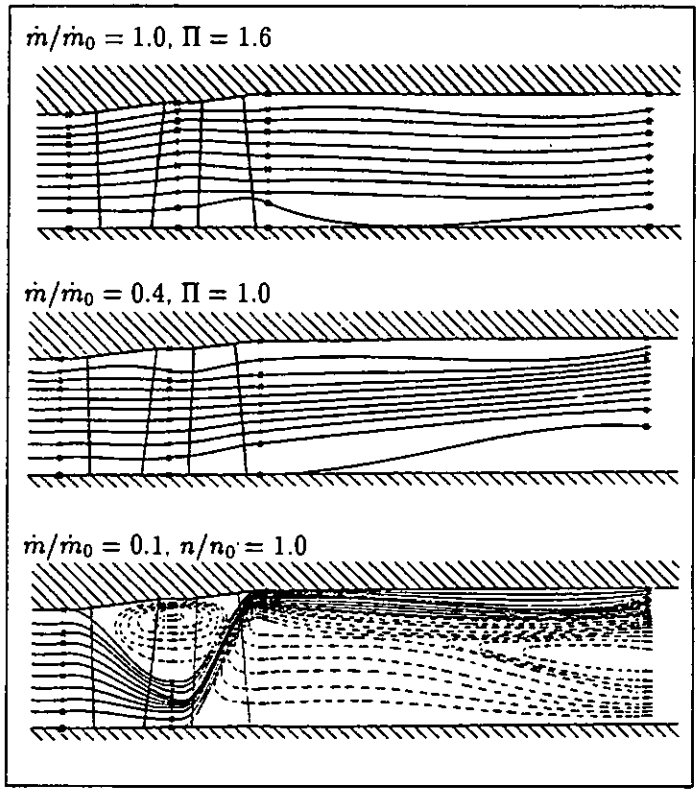

Fig. 1 - Streamlines in meridional surface of the single-stage experimental turbine at design load and two part loads plotted according to the experimental data

Flow phenomena and turbine behavior at part loads were extensively investigated at an air turbine at the Institute for Turbomachinery, Hanover. The experimental turbine blading of the Institute may be changed to single-stage, two-stage and four-stage configuration. Radial distribution of representative flow values is determined by radial probe traverses in suitable positions. Since the pneumatic five-hole probe was used, only the average value of the measured parameters could be acquired. Possible unsteady effects were not analyzed.

Figure 1 shows results of experiments for single-stage blading (Riess and Evers, 1985). The turbine flow field is presented by meridional streamlines for different mass flow rates, $\dot{m}/\dot{m}_0$ at nominal rotating speed $n/n_0 = 1.0$ The first slow separation

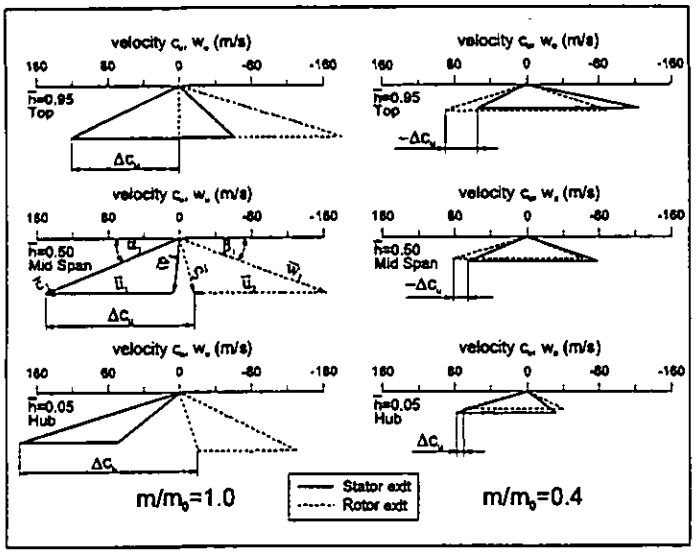

Fig. 2 - Calculated velocity triangles of single-stage turbine for design load and one part load

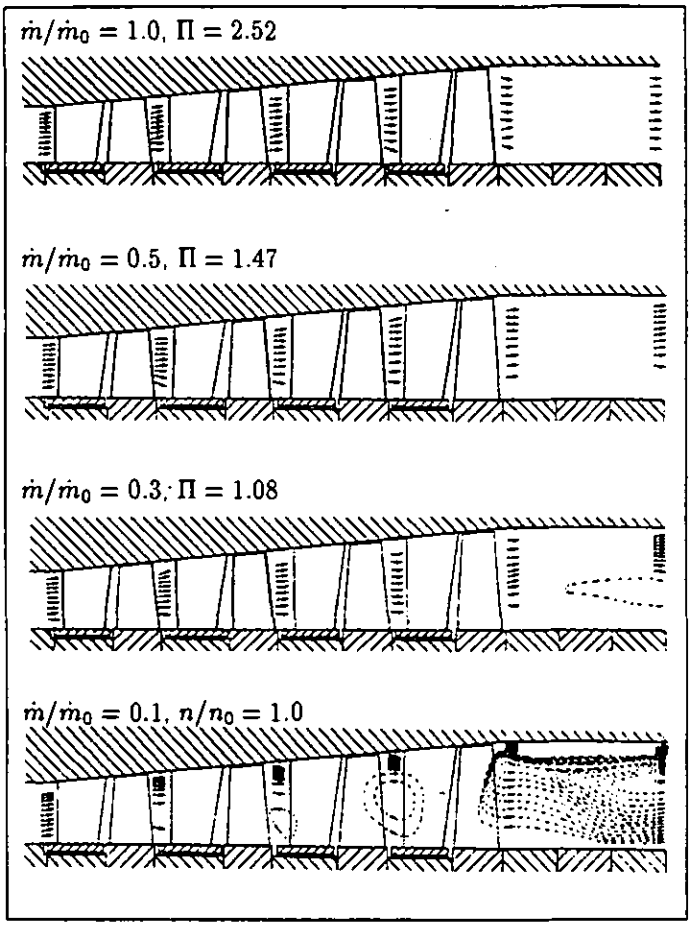

Fig. 3 - Streamlines within meridional surface of the four-stage experimental turbine at design load and three part loads plotted according to the experimental data

was detected in the hub region behind rotor at about 40% of nominal mass flow ($\dot{m}/\dot{m}_0 = 0.4$). In case of further reduction of mass flow, reversal in outlet diffuser increases and flow separation extends to the gap between stator and rotor. At $\dot{m}/\dot{m}_0 = 0.1$, flow field consists of two large vortices and a narrow band of active flow, diagonally traversing the rotor.

The shape of a streamline, along which fluid particle moves, is a function of flow channel form and forces, which act on the particle. The forces always stand in equilibrium. For example, if friction forces are neglected, in turbine outlet diffuser two forces act in radial direction: a centrifugal force and a surface force due to radial pressure gradient (pressure force). In most cases, the last stage of the turbine is designed in such a way that, circumferential component of absolute velocity is very small and pressure along the span is almost constant at the rotor exit at nominal conditions. Centrifugal and pressure forces are in equilibrium at approximately equidistant streamlines (Fig. 1). At part loads, circumferential component of absolute velocity at the rotor exit and the centrifugal force increase. Streamlines move in radial direction. In the boundary case, fluid particles cannot follow the hub satisfying equilibrium between centrifugal and pressure forces, thus causing flow separation. In case of further reduction of volume flow, centrifugal force increases and region with reverse flow in outlet diffuser grows.

Appearance of vortex in an axial gap between stator and rotor may be accounted for in a similar fashion. Here, at low loads, circumferential component of absolute velocity and centrifugal force decrease, since the volume flow is reduced. Therefore, flow separation and vortex occur in the top region. Figure 2 shows velocity triangles for three characteristic sections of single-stage turbine: near hub, mid span and near top for nominal load and one part load ($\dot{m}/\dot{m}_0 = 0.4$, $\Pi \approx 1.0$). The change in circumferential component of absolute velocity causes not only flow separation, but the decrease stage capability to generate mechanical work. It may be seen that at load with $\dot{m}/\dot{m}_0 = 0.4$, flow parameters change so much that, at mid span and in top region, Δc_u and aerodynamic work become negative. It means that rotating blades transmit energy to the fluid and this part of stage works as a compressor while the hub region of the stage still produces work ($\Delta c_u > 0$).

Results of flow measurement in four-stage experimental air turbine, for nominal and a few part loads are shown in Fig. 3. It may be seen that, at part loads, the last stage of the multistage turbine behaves similarly to the single-stage one.

The extensive investigations of flow in LP steam turbines, which have been performed at the Institute for Turbomachinery, have confirmed the existence of flow separations and reversal at part loads behind the last stage of the LP part. The shape of this vortices is similar to the ones which were determined in the experimental turbine. Figure 4 shows distribution of meridian velocity in the measuring plane behind the last stage of LP part 165 MW steam turbine at part load with volume flow $\dot{V} = 0.37\dot{V}_0$ (Schmidt, Riess, 1995).

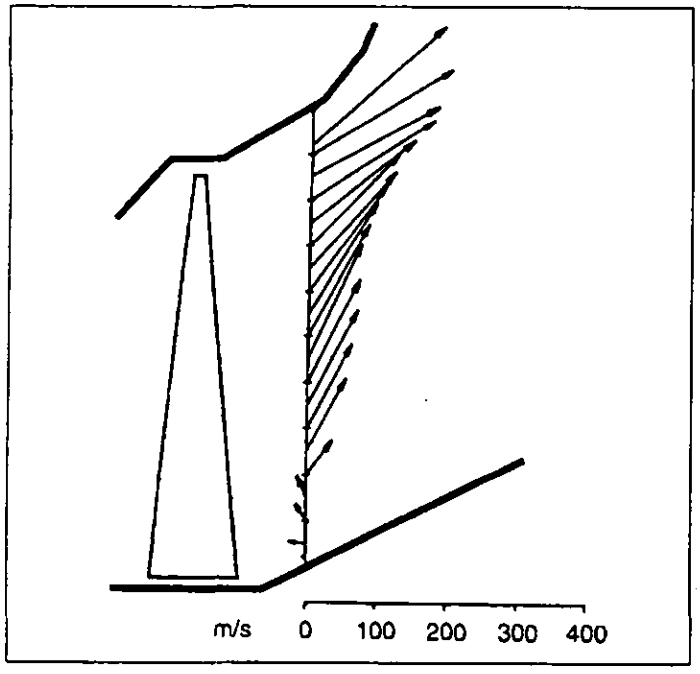

Fig. 4 - Distribution of meridian velocity in the measuring plane behind the last stage of LP part 165 MW steam turbine at part load with volume flow $\dot{V} = 0.37\dot{V}_0$

CALCULATION METHOD

Analytical Background

The purpose of the work presented here is to develop computing system for flow analysis and performance prediction of multistage gas and steam turbines over a wide range of speed and load. The analysis of far off-design operation with flow separation and loads, at which the turbine or some stages start to work with power consumption, should also be encompassed. Two conditions were set: computing system should be quick enough for economical flow analysis, parameters variation and optimization in design phase, and the assumed level of approximations should not disturb the desired high accuracy of procedure.

The method has been developed on the basis of classical through-flow theory primarily using the analyzes of Hirsch and Deconinck (1985) and Bosman and Marsh (1972), but it includes new details and extensions. The flow is assumed to be steady, adiabatic and axisymmetric, by which a two dimensional description is achieved. The 2D calculation is made within the meridional hub-to-shroud surface, at which the momentum equation is projected. Body forces are introduced to replace turbine blades. Flow loss effects are approximated by a friction force.

The resulting momentum equation has the following form:

$$\frac{\partial^2\psi}{\partial r^2} + \frac{\partial^2\psi}{\partial z^2} = \left[\frac{2\pi}{\dot{m}}q - \frac{\partial\psi}{\partial r}\frac{\partial}{\partial r}\left(\frac{1}{\rho rb}\right) - \frac{\partial\psi}{\partial z}\frac{\partial}{\partial z}\left(\frac{1}{\rho rb}\right)\right](\rho rb), \qquad (1)$$

where q is the function of the turbine geometry, velocities and fluid properties distribution (Hirsch and Deconinck, 1985).

Stream function is defined with relations:

$$\frac{\partial\psi}{\partial r} = \frac{2\pi}{\dot{m}}\rho rb\, w_z, \qquad \frac{\partial\psi}{\partial z} = -\frac{2\pi}{\dot{m}}\rho rb\, w_r, \qquad (2)$$

where: $\dot{m}$ is the mass flow rate and b is the tangential blockage factor ($b = 1 - d/t$, d is the tangential blade thickness and t is the blade pitch).

The mass flow $\dot{m}$ is introduced in the stream function equations since it makes the definition of boundary conditions easier. Namely, boundary conditions for turbines without extractions are defined as: $\psi = 0.0$ along the hub and $\psi = 1.0$ along the shroud, and, since $\dot{m}$ is included in Eq. (2), they remain constant during calculations for the whole turbine operating range: nominal and part loads. In case of turbines with extraction,the value of the stream function in calculating points at the shroud downstream of extraction locations has to be reduced according to the extracted mass flow rate.

By solving momentum equation (1) with the introduction of continuity equation, energy equation and equation of state, the velocity vector and the thermodynamic state of the working fluid are obtained. The loss model is applied to calculate the entropy variation, while the deviation model is applied to determine circumferential component of the flow velocity. Based on the calculated flow field, the overall performance of the turbine and parameters of separate stages may be obtained.

Gas Properties and Density Calculation

In order to attain as higher accuracy of the present procedure as possible, working fluid is assumed to be real gas. To calculate steam properties an equation for free energy $f = f(\rho, T)$ (Saul, 1988) is used, which enables very accurate computation. For air and combustion gases, Baehr's and Diedrichsen's (1988) correlations are applied.

At calculating the flow parameters in a point of grid values of H, s, c_u are known. The total enthalpy H remains constant along a streamline within stator and duct regions (the rothalpy I is constant along a streamline within a rotor). The entropy s is obtained using the loss model, while the circumferential velocity component c_u is determined using deviation model. Unknown are the density ρ and the meridional velocity components, w_z and w_r, which have to be computed.

Since the real gas model is applied, the procedure developed by *Hirsch* (Hirsch, Deconinck, 1985), where the correlations for perfect gas were used, could not be applied. Because of that, new similar procedure was developed.

The equation valid for static enthalpy is the following:

$$h = H - \frac{c^2}{2}. \qquad (3)$$

Using the definition of stream function (Eq. 2) the velocity may be written as:

$$c^2 = c_z^2 + c_r^2 + c_u^2 = \frac{\dot{m}^2}{(2\pi\rho rb)^2}\left[\left(\frac{\partial\psi}{\partial r}\right)^2 + \left(\frac{\partial\psi}{\partial z}\right)^2\right] + c_u^2 \qquad (4)$$

and with:

$$A = \frac{1}{2}\frac{\dot{m}^2}{(2\pi br)^2}\left[\left(\frac{\partial\psi}{\partial r}\right)^2 + \left(\frac{\partial\psi}{\partial z}\right)^2\right], \qquad B = \frac{c_u^2}{2}, \quad (5)$$

Eq. (3) takes the following form:

$$h = H - \frac{A}{\varrho^2} - B. \quad (6)$$

Since the function $\varrho = f(h, s)$ is known and the values of parameters A and B may be estimated using the starting distribution of stream function, Eq. (6) becomes

$$h = H - \frac{A}{\left[\varrho(h,s)\right]^2} - B = f(h). \quad (7)$$

Applying a simple iterative process to solve Eq. (7), the static enthalpy h may be determined. Value $h = H$ is used as the starting value. The process converges quickly and only a few iteration steps are necessary. Since the entropy s is known, the density ϱ is obtain using the function $\varrho = \varrho(h, s)$. The axial and the radial velocity components, w_z and w_r, are computed using the stream function definition (Eq. (2)).

Method of Solution

The governing through-flow equation (1) is a second order, quasi linear partial differential equation. It is elliptic for subsonic meridional flow elliptic and it may be solved iteratively using discretisation on a fixed grid. Here, the finite element method with eight-node isoparametric quadrilateral elements and biquadratic interpolation functions, is used. The Galerkin procedure of weighted residual is applied to form the finite element equations, while the frontal solving method is used to solve the resulting system of linear equations. The computer program was written in FORTRAN, the IBM RISC 6000 Workstation was used for calculations.

LOSS MODEL

Prediction of Losses at the Design Conditions

For the loss coefficient prediction and the entropy increase estimation at the design operating point, Traupel's loss model (Traupel, 1988) was applied. Traupel presents the loss coefficient as functions of geometric and flow parameters in form of several diagrams. For present calculations these functions are approximated with polynomials (Petrovic, 1995). Loss coefficient ζ is defined as: $\zeta = 1 - w_2^2/w_{2s}^2$, where: w_2 is the real velocity and w_{2s} is the isentropic velocity at blade row exit.

Radial Distribution of Loss Coefficient

At common through-flow calculation in axial turbines, the profile loss coefficient at any radius r is determined according to local flow and geometrical parameters. The secondary and the clearance loss coefficients are determined for the flow at mean radius and uniformly distributed along the blade height, although

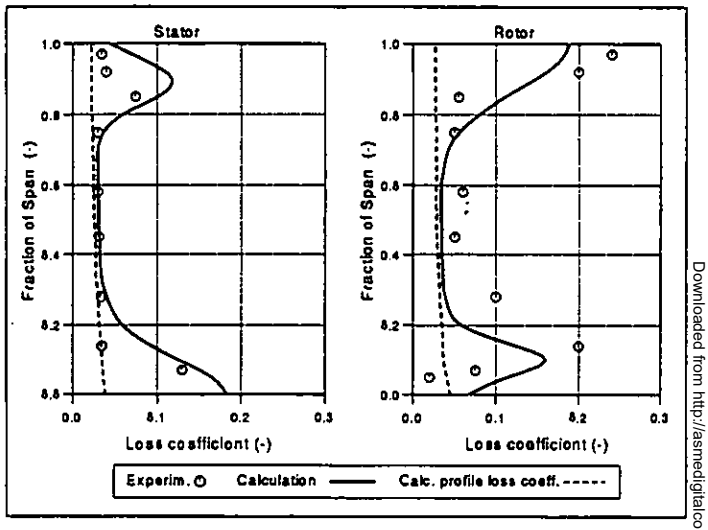

Fig. 5 - Radial distribution of loss coefficient for stator and rotor of the experimental single-stage turbine under design operating conditions

these losses are concentrated only in the hub and tip region. In order to take this into consideration a new model for radial loss distribution is applied. It is based on the extensive experimental investigation of different stage geometry and flow conditions performed by Groschup, (1977) and further developed by Petrovic and Riess (1995).

The model assumes that secondary and clearance losses are concentrated in the hub and shroud region of blade rows, whose width is determined using Traupel's correlation (Traupel, 1988):

$$\Delta\bar{h} = (3 \div 5)\frac{t}{h}\sqrt{\zeta_P}, \quad (8)$$

where t is pitch, h is blade height and ζ_P profile loss coefficient calculated for parameters in the middle of the region.

For the distribution of secondary and clearance loss coefficient function e^{x^2} is selected. The total loss coefficient at the relative blade height $\bar{h}$ may be expressed by:

$$\zeta(\bar{h}) = \zeta_P(\bar{h}) + B_H\, e^{-A_H(\bar{h}-C_H)^2} + B_T\, e^{-A_T(1-\bar{h}-C_T)^2}, \quad (9)$$

where $\zeta_P(\bar{h})$ is the local profile loss coefficient.

The last two terms represent the spanwise variation of secondary and clearance loss coefficients. Function e^{x^2} provides distribution along the whole blade height, but decreases very quickly with x and asymptotically tends to zero. Positions in hub and tip region, at which function (9) reaches maximum, are defined by C_H and C_T. According to Groschup, on the side of flow channel near the clearance the maximum lies at the edge of the boundary, and at the opposite side it lies in the center of the secondary flow region determined in Eq. (8). This means that for stator blade rows the values are: $C_H = 0$, $C_T = \Delta\bar{h}_T/2$, and for rotor blade rows: $C_H = \Delta\bar{h}_H/2$, $C_T = 0$. Factors A_H and A_T present the quotient between values of the distribution function

at the boundary of the secondary flow region and maximum values of the distribution function. According to the experiments by Groschup, $A_H = A_T = 0.1$ was assumed.

The total value of the secondary and clearance loss coefficients which should be distributed in hub and tip region of stator is:

$$\zeta_H^* = 0.5 \cdot \zeta_{S,H} + 1.0 \cdot \zeta_{Cl}, \qquad \zeta_T^* = 0.5 \cdot \zeta_{S,T}, \qquad (10)$$

where $\zeta_{S,H}$ and $\zeta_{S,T}$ are secondary loss coefficients calculated for parameters in the center of the hub, and tip secondary flow region respectively. For the rotor, the clearance loss coefficient has to be added to the tip secondary flow region ($\zeta_T^* = 0.5 \cdot \zeta_{S,T} + 1.0 \cdot \zeta_{Cl}$).

Values of factors B_H and B_T may be obtained according to Eq. (9) and Eq. (10). For example, in case of the stator:

$$B_H = \frac{\zeta_H^*}{\int_0^1 e^{-A_H(\bar{h}-C_H)^2} d\bar{h}}, \quad B_T = \frac{\zeta_T^*}{\int_0^1 e^{-A_T(1-\bar{h}-C_T)^2} d\bar{h}}. \qquad (11)$$

Figure 5 shows results of loss coefficient calculation according to the presented model for stator and rotor blade rows of the single-stage air turbine at nominal load with incidence angles near zero, as well as comparison with experimental data.

Loss Coefficient Prediction at Part Load

The accuracy of flow calculation and prediction of turbines performances at part load depend very much on the ability of the loss model to determine the loss coefficient at this load correctly. The models by Traupel (1988) and by Ainley and Mathieson (1957) are the most frequently used ones. In both cases the loss coefficient is given as a function of the incidence angle. The functions are of a parabolic character and increase very quickly at higher incidence. In this work model by Zehner (1980) is used.

Zehner investigated experimentally the flow characteristics of many plane cascades with different geometry, changing the inlet flow angle from 0° to 180°, i.e. taking into consideration all possible incidence angles. Based on the experimental data, he developed correlation for calculating the off-design profile loss coefficient, in the form:

$$\zeta_P = 1 - (1 - \zeta_{P0})\, e^{-a(\Delta\beta^*)^b}, \qquad (12)$$

where ζ_{P0} is the profile loss coefficient at design conditions and $\Delta\beta^*$ is the non-dimensional function of the incidence angle $\Delta\beta$. Coefficients a and b in Eq. (12) are empirical functions the cascade parameter γ, introduced by Zehner in the form (Zehner, 1980):

$$\gamma = \frac{f}{t}\sqrt{\beta_s \cdot \delta}, \qquad (13)$$

where f is the height of the camber line, t is the pitch, β_s is the stagger angle and δ is the deflection angle ($\delta = 180 - (\beta_1 + \beta_2)$). The angles β_s and δ are given in radians.

The secondary and the clearance loss coefficients at part load are calculated using the same correlations as for nominal load, but under the new flow conditions. The effect of the model is presented in Fig. 6 with the example.

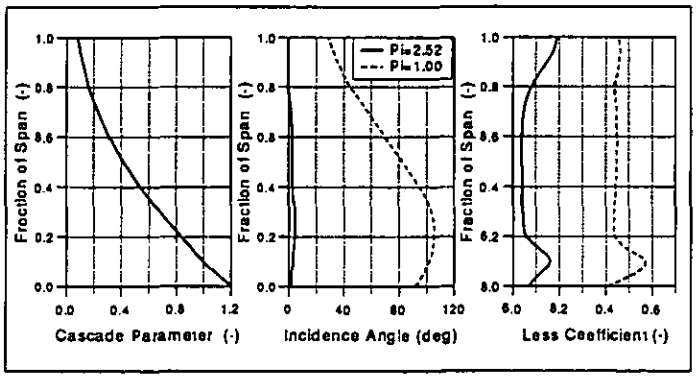

Fig. 6 - Effect of the applied model for part load losses calculation on the loss coefficient of rotor blade row of single-stage experimental turbine

SPANWISE MIXING

Through-flow methods which relate to realistic model of the radial loss distribution, should include a model for mixing endwall and main flows, in order to avoid unreal accumulations of entropy increases in end-wall regions. Spanwise mixing at through-flow calculation is simulated by allowing transfer of enthalpy, entropy and angular momentum between streamlines. For the flow calculation in compressors, mixing models by Adkins and Smith (1981), and Gallimore (1986) are mostly used. Based on these two approaches, Lewis (1994) published the model for spanwise mixing in axial flow turbines. For the present calculation, we developed and applied a simple mathematical model for spanwise mixing, easy to be implemented in through-flow procedure, and we got good results.

Mixing within the blade rows and mixing in axial ducts are handled separately. The spanwise mixing model assumes that mixing effects within the blade row are already included in the model for radial loss distribution, since it is developed on the basis of experimental data and gives loss distribution at the outlet of the blade row. Additional spanwise mixing occurs in axial ducts between the blade rows and turbine outlet diffuser, and should be handled separately. The said process is modeled by redistribution of values of s, H and rc_u in all nodes in ducts.

During the flow calculation in an axial duct, in all nodes lying at the duct exit, values of s, H and rc_u are at first estimated as if there was no mixing (original distribution "o"). Then, these values are approximated with a spline function, and new values distributed in all calculated nodes at the duct exit (new distribution "new"). The proportion factor of the selected spline polynomial (Engeln-Muellges and Reutter, 1988) is chosen in a way that the extreme values of original distribution curves of s, H and rc_u at exit of an axial duct are reduced by 50% compared to the linear approximation of the original distribution. The new distributions of the s, H and rc_u have the same integral values over the mass flow as the original one: $\int_0^1 s_o d\psi = \int_0^1 s_{new} d\psi$, $\int_0^1 H_o d\psi = \int_0^1 H_{new} d\psi$, $\int_0^1 rc_{u,o} d\psi = \int_0^1 rc_{u,new} d\psi$, but have smaller gradients. The changes of values s, H and rc_u along a streamline from the duct inlet to the duct outlet are linearly distributed. The influence of the applied mixing model on flow parameters is controlled by comparing calculations with experimental data.

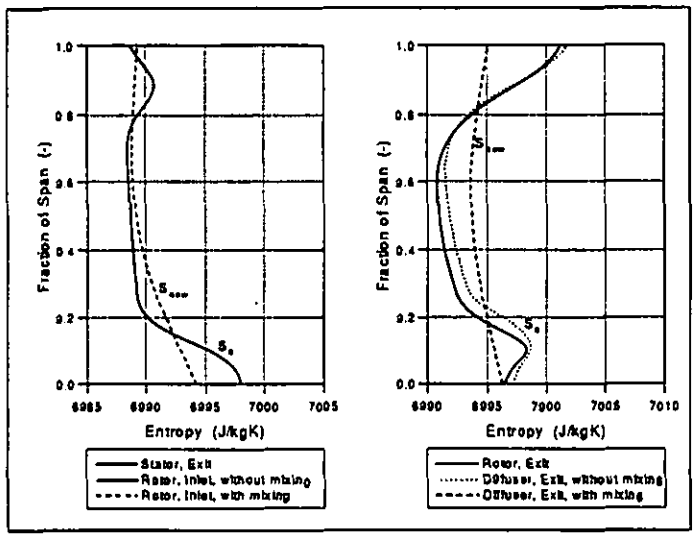

Fig. 7 - Effect of the applied spanwise mixing model on entropy distribution in the single-stage turbine at design load

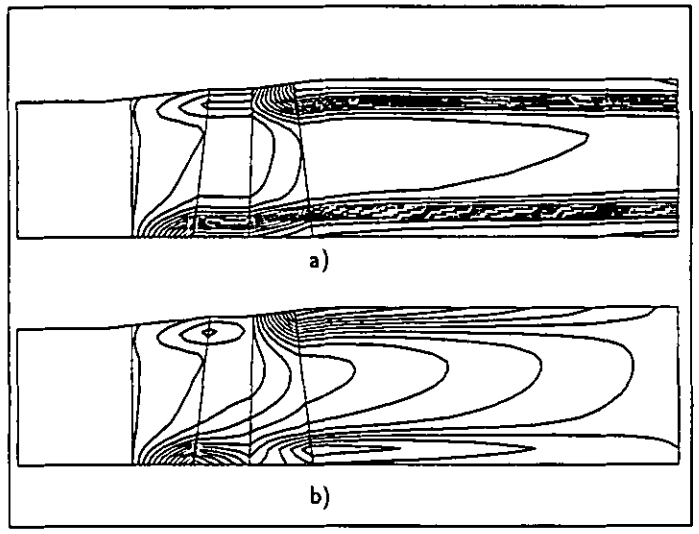

Fig. 8 - Entropy distribution in the single-stage turbine at design load: a) – calculation without spanwise mixing model, b) – by applying spanwise mixing model. The increment between isolines is $1J/kgK$

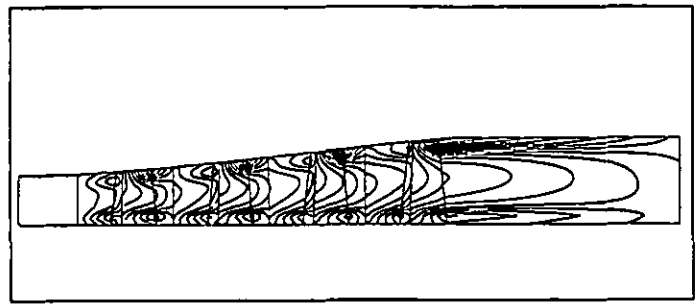

Fig. 9 - Calculated entropy distribution in the 4-stage experimental turbine at design load

Figure 7 shows effect of the applied mixing model on the entropy distribution in axial duct between stator and rotor and in outlet diffuser of the experimental single-stage turbine. Calculated entropy distributions in both single-stage and four-stage experimental air turbines are shown in Fig. 8 and 9.

The implementation of the spanwise mixing model in through-flow procedure is very easy. The model is reliable and gives good results for the flow calculations in LP steam turbine with high Mach numbers as well. Neglected is The increase of calculating time is neglected because the the spanwise mixing model. Presently, we are working on a paper which will provide detailed comparisons of the measuring data and numerical results obtained through the application mathematical mixing model and the other known models.

DEVIATION MODEL

For calculating cascade exit flow angle, a new correlation in form of corrected sine rule ($sin\beta_2 = a/t$, where a is throat width and t is blade pitch) is developed. The deviation of the exit flow angle is assumed to be proportional to the local value of the secondary and clearance loss coefficients, ζ_S and ζ_{Cl}:

$$\beta_2 = asin\Big(K_a \frac{1}{\sqrt{1+\zeta_S+\zeta_{Cl}}} \frac{a}{t}\Big) + K_y, \qquad (14)$$

where β_2 is calculated in degrees. Factor K_y considers the additional deviation in the wet steam region:

$$K_y = 20y_1, \qquad (15)$$

where y_1 is the wetness fraction at cascade inlet and K_a is the correcting factor for supersonic flow (Shcheglyaev, 1976):

$$K_a = \left[\frac{2}{\kappa-1}\Big(\frac{\kappa+1}{2}\Big)^{(\kappa+1)/(\kappa-1)}\Big(\varepsilon^{2/\kappa} - \varepsilon^{(\kappa+1)/\kappa}\Big)\right]^{1/2}, \qquad (16)$$

where ε is the cascade pressure ratio: $\varepsilon = (p_2/p_1^0)$ with $p_1^0 = f(s_1, h_1 + w_1^2/2)$ for rotor and $p_1^0 = f(s_1, h_1 + c_1^2/2)$ for stator (1 – cascade inlet, 2 – cascade outlet). For subsonic flow is $K_a = 1.0$.

Fig. 10 shows flow angles at the single stage experimental turbine stator and rotor exit calculated according to Eq. (14).

APPLICATION OF THE METHOD

On the basis of the presented model,a computer program for through-flow calculation in axial flow turbines was developed. For the development of the code, test calculations and validation of the applied methods,used were the data on the single-stage and 4-stage experimental air turbine at the Institute for Turbomachinery, Hanover. Two LP steam turbines, for which measurements of the flow distribution are available, were analyzed to assure reliability of the code and to determine its limitations. The method may be applied for flow analysis in gas and steam turbines for a very wide range of loads and for subsonic and trasonic flow. The calculation reported here relates to the 4-stage experimental turbine.

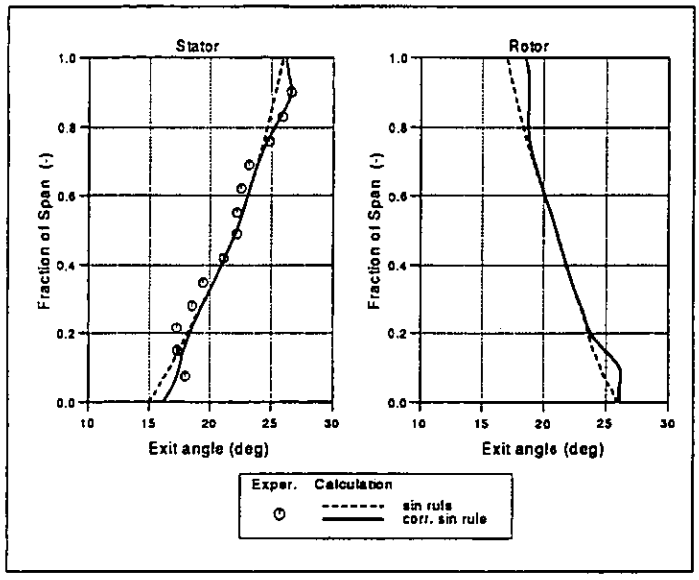

Fig. 10 - Radial variation of the single-stage experimental air turbine exit flow angles

EXPERIMENTAL 4-STAGE AIR TURBINE

Figure 11 shows longitudinal section of the experimental air turbine in four-stage configuration. The design data for the turbine are given in Table 1.

The facility was basically designed to have the same blade sections in each stages, at the given radius. Blading is of free vortex type with 50% degree of reaction in the middle section of the last stage. Views of stator and rotor blade profiles are given in Fig. 11. The form and aerodynamic loading of blading are not exactly similar to those of an LP steam turbine or a power gas turbine, since the peripheral speed and the Mach number are considerably lower. Nevertheless, the relative blade length, blade twist and distribution of reaction are sufficiently typical and therefore suitable for investigation of the flow at both design and off-design conditions.

The turbine is supplied with air, compressed by three screw compressors and coupled via gearbox with DC pendulum-type machine. The rotation speed can be adjusted by voltage control, while air flow rate may be set using the by-pass. Blading may be changed to a single-stage or two stage configuration.

Table 1 - Design data of four-stage turbine

Power output	P_i	=	703.0	kW
Speed	n_0	=	7500	rpm
Air flow rate	$\dot{m}_0$	=	7.8	kg/s
Inlet pressure	p_{in}	=	2.600	bar
Inlet temperature	t_{in}	=	413.0	K
Outlet pressure	p_{out}	=	1.022	bar
Hub diameter	D_H	=	270	mm
Hub ratio at outlet	D_H/D_T	=	0.525	$-$

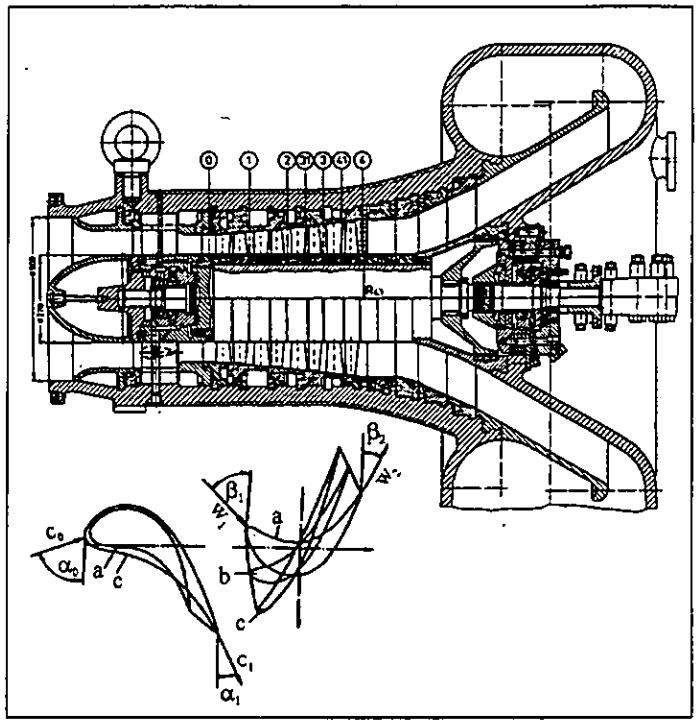

Fig. 11 - Cross-section of experimental air turbine of the Institute for Turbomachinery, Hanover and profiles of stator and rotor blade at hub (a), mean radius (b) and shroud (c) section with flow angles and velocity triangles definition.

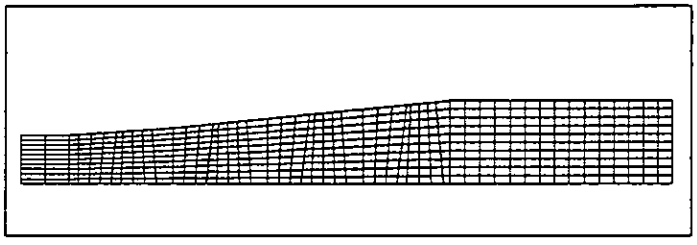

Fig. 12 - Finite element distribution of 4-stage experimental turbine

ANALYSIS OF 4-STAGE EXPERIMENTAL TURBINE

Flow calculations were performed for nominal load and several part loads, for which experimental data had been available. The input data for flow calculation of every individual load are: turbine geometry, rotation speed, inlet temperature, inlet and outlet pressure. The mass flow rate is obtained iteratively. Two different rotation speeds are considered: the nominal $n_0 = 7500rpm$ and a lower speed $n = 0.75n_0 = 5625rpm$. The variation of the inlet total temperature during experiments was not to large, and consequently, the reduced speeds $n/\sqrt{T}$ were approximately constant for each of the two speeds. The inlet pressure was varied from nominal value $p_{in,0} = 2.6bar$ to $p_{in} = 1.0bar$. Calculated domain with element distribution of the turbine is shown in Fig.

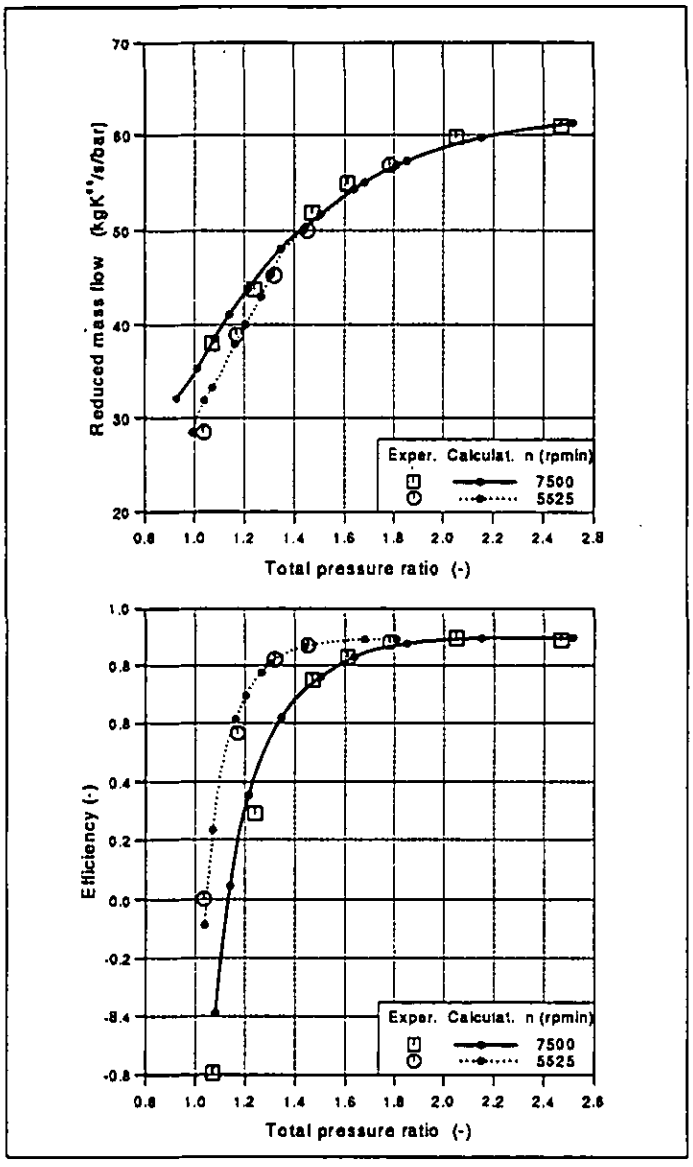

Fig. 13 - Overall performance of 4-stage turbine

12. The grid refinements study was performed to make computing time shorter. It was concluded that the use of ten elements in the radial direction and three per blade row in the axial direction, gives very good results.

Figure 13 shows diagrams with calculated turbine overall performance and the comparison with experimental results. The turbine performances are given as functions of reduced mass flow $\dot{m}\sqrt{T_{in}}/p_{in}$ and turbine efficiency η_{ts} from the pressure ratio. Pressure ratio is defined as the relation between total pressures at the turbine inlet and outlet: $\Pi = p^o_{in}/p^o_{out}$ and η_{ts}n is internal isentropic total to static efficiency.

The agreement between numerical values of the reduced mass flow and experimental data is very good: the test values practically lay on the predicted curves. At the nominal rotation speed at $\dot{m}\sqrt{T_{in}}/p_{in} \approx 35 kgK^{0.5}/s/bar$, pressure ratio Π approaches

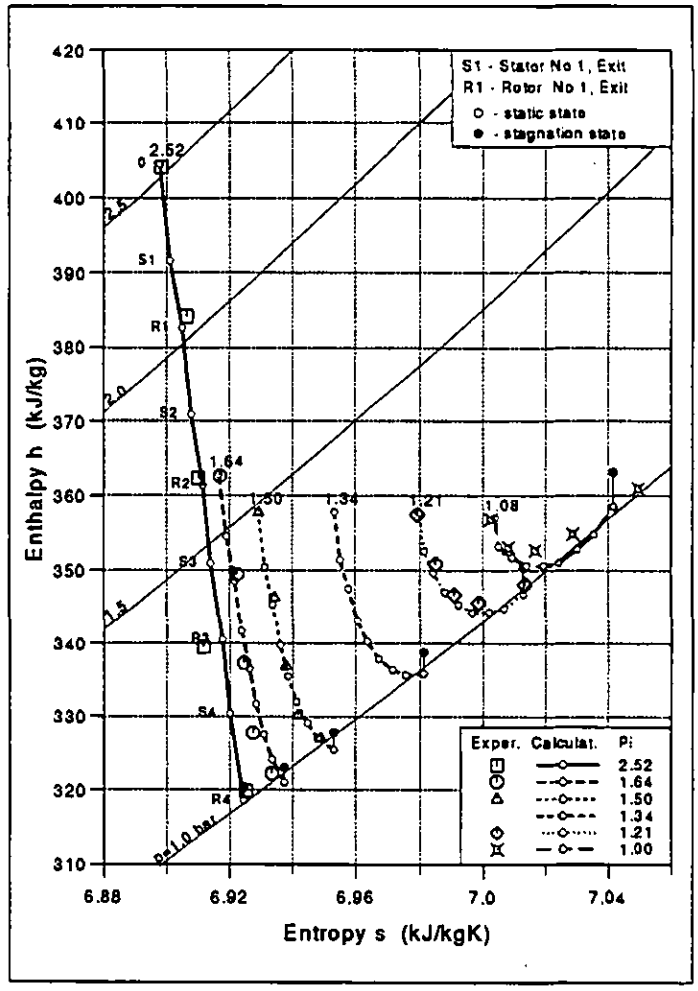

Fig. 14 - Expansion in 4-stage turbine at $n_0 = 7500rpm$

1.0. At a smaller mass flow rates the pressure is higher at the turbine exit than at the inlet, and it operates as a compressor.

By reducing the pressure ratio from the design value $\Pi = 2.52$ to $\Pi \approx 1.6$ at the nominal speed, the turbine efficiency slightly decreases and, later it decreases very quickly. At $\Pi \approx 1.15$ the efficiency approaches zero, $\eta_{ts} = 0$. It means that under this conditions, the turbine starts to work with power consumption.Negative value of η_{ts} at $\Pi > 1$ indicates that, in spite of small expansion of gases, the turbine internal work at this load is negative, since flow losses are larger than the available isentropic enthalpy drop. In case of loads, at which the pressure is higher at the turbine outlet than at the turbine inlet the calculation of efficiency has no sense.

Figure 14 shows h, s-diagrams with calculated turbine expansion lines for the nominal load ($\Pi = 2.52$) and for several part loads. The agreement between predicted curve and experimental results is very good. The expansion lines are created with thermodynamic state of the air, averaged over the mass flow. At the nominal load, the enthalpy drop is evenly divided into stages. By reducing the pressure ratio and the mass flow, the stage enthalpy differences decreased.

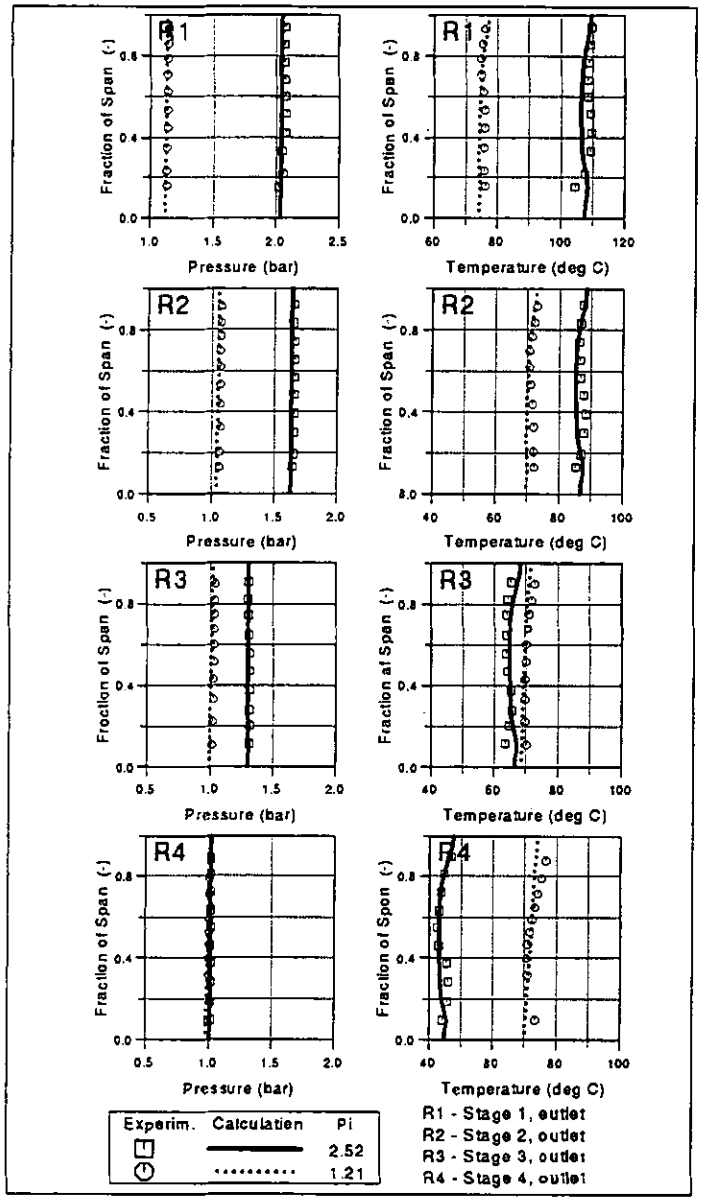

Fig. 15 - Measured and calculated radial profiles of pressure and temperature through 4-stage turbine at design load ($\Pi = 2.52$) and at one part load ($\Pi = 1.21$) at $n = 7500rpm$

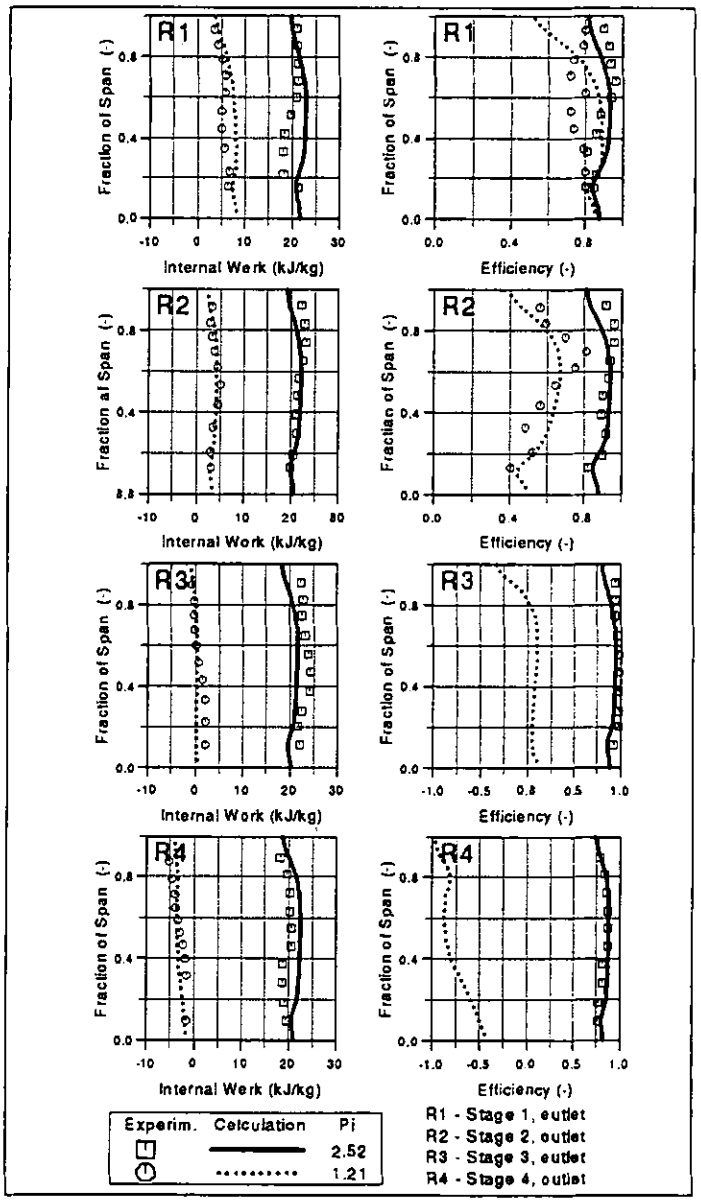

Fig. 16 - Measured and calculated radial profiles of internal work and efficiency of stages of 4-stage turbine at design load ($\Pi = 2.52$) and at one part load ($\Pi = 1.21$) at $n = 7500rpm$

At $\Pi = 1.34$, there is no expansion in the last stage, $\Delta h_4 \approx 0$. In case of further reduction of the pressure ratio the stages, beginning at the last rotor, change to operation with power consumption. At $\Pi = 1.21$, the enthalpy of the working fluid is increased in the last turbine stage. The expansion in the 3rd stage is very small. The turbine efficiency is still positive (Fig. 13) since the internal work, produced by the first three stages, is larger than the work consumed by the last one. At $\Pi = 1.08$, the gas is expanded in the first two stages and it is compressed in last two ones. The turbine efficiency is negative.

Figure 15 shows radial distribution of pressure and temperature at the exit of rotating blade rows. Radial profiles of stage parameters, specific internal work, and efficiency are presented in Fig. 16. Calculation results and experimental data for nominal load ($\Pi = 2.52$) and for one typical low load ($\Pi = 1.21$) are presented. It may be seen that the correspondence between calculations and measurements is good. even at part load. At $\Pi = 1.21$, the stage internal work decreases. In the third stage the work within hub part of blade is positive, while within the top one it is negative. Internal work along the whole hight of the last stage, as well as the efficiency, are negative.

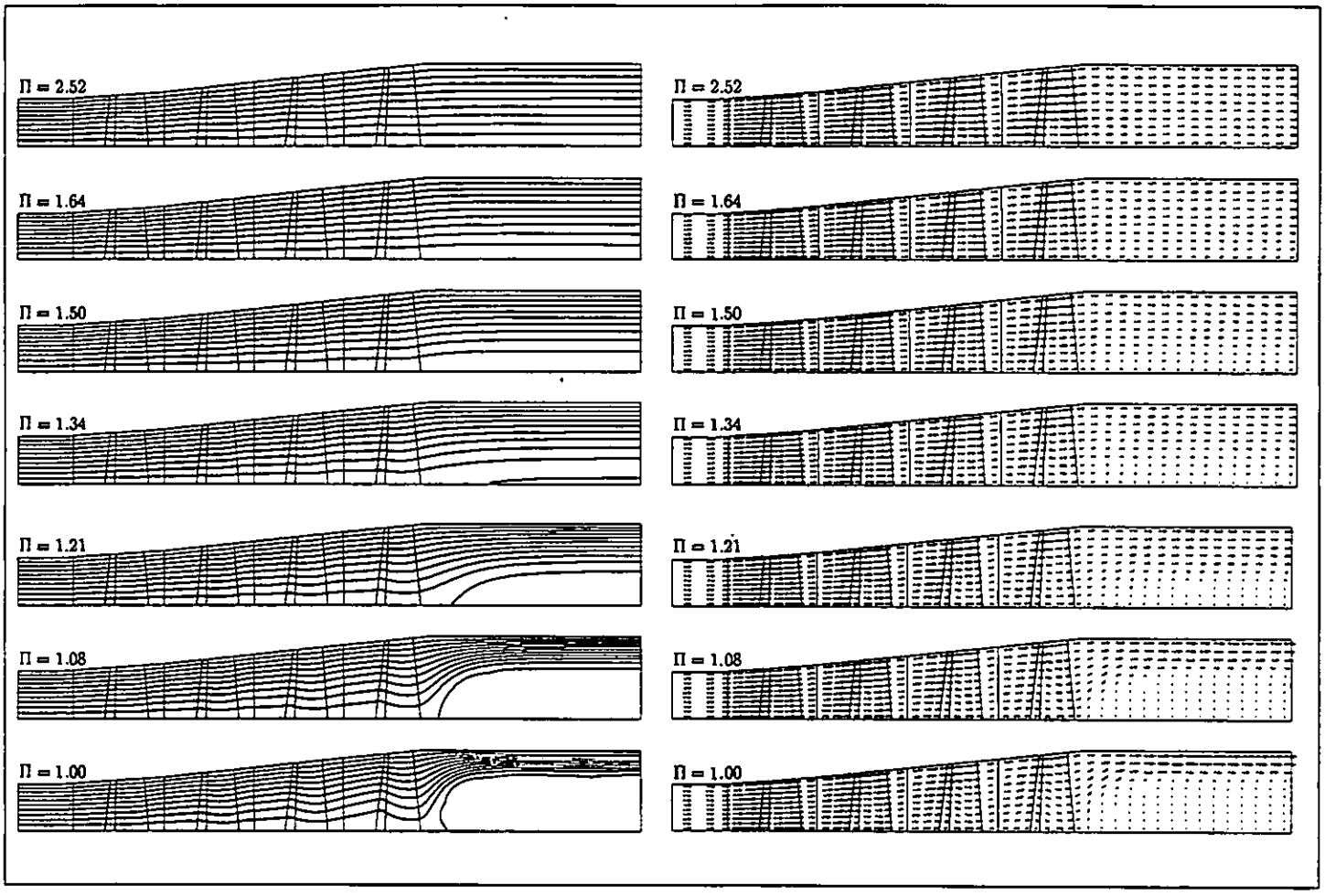

Fig. 17 - Streamlines and velocity vectors in meridional surface of 4-stage experimental turbine at design load and at several part loads

The complete flow field of the turbine is obtained through flow calculation. It is given as the meridional surface distribution of the following parameters: temperature, pressure, enthalpy, entropy, velocity components, stream function, Mach number etc. Based on the flow field, the overall performance of the turbine and different operating parameters of stages may be estimated. Figure 17 shows some results of the flow field calculation: streamlines and velocity vectors in the meridional surface for design operation and for several part loads. The flow separation and the flow reversal in hub region behind the last rotating blade row are detected at $\Pi = 1.34$ ($\dot{m}/\dot{m}_0 = 0.45$) first. The reverse flow region grows by reducing the pressure ratio and the mass flow rate. The meridional components of velocities in flow reversal are small, and consequently, only a small fraction of the mass flow streams within this region. The results of calculation of reverse flow region height and comparison to measuring data for plane at diffuser outlet, are shown in Fig. 18. The flow field of the 4-stage turbine, plotted according to experimental data, is shown in Fig. 3. The calculations of flow at loads with $\Pi < 1.0$ ware not possible, due to numerical instability, caused by vortices, which appear in axial ducts between blade rows at low volume flow.

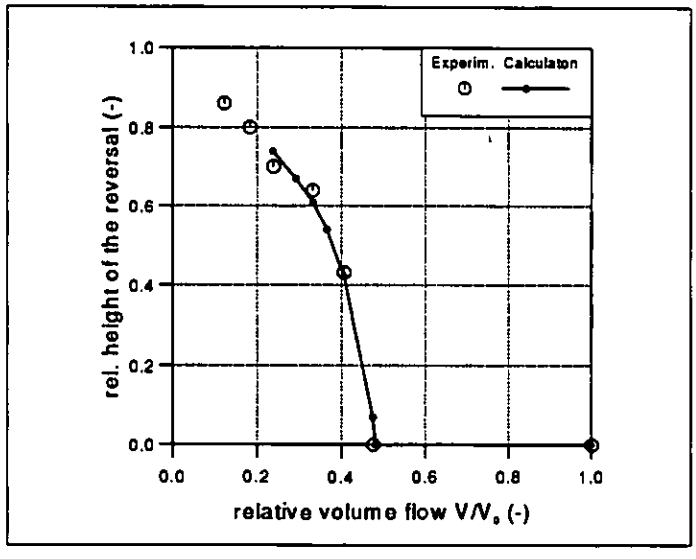

Fig. 18 - The height of reverse flow region in 4-stage experimental turbine

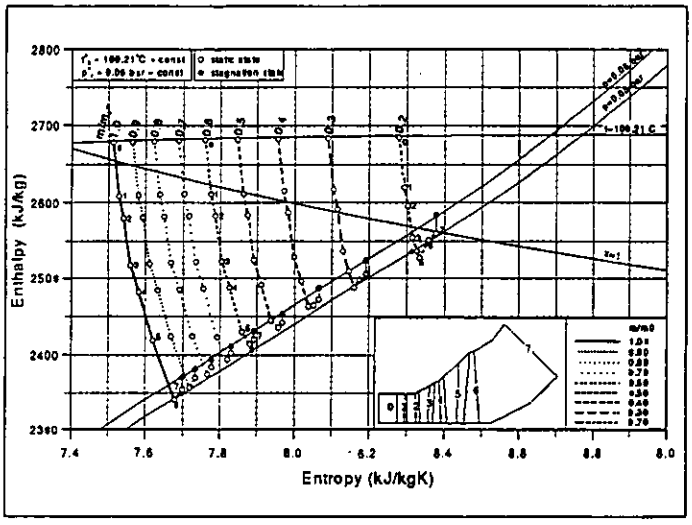

Fig. 19 - Expansion in 3-stage LP-part of 165 MW steam turbine

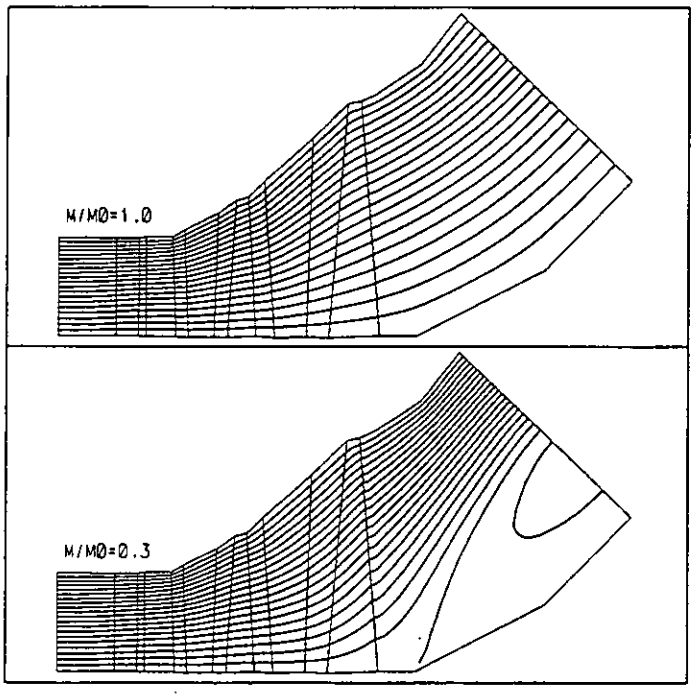

Fig. 20 - Streamlines in meridional surface of LP-part of 165 MW steam turbine at design load and one part load

STEAM TURBINE FLOW CALCULATION

For program development and validation of the applied methods, test calculations of flow in LP-parts of two different steam turbines (350 MW and 165 MW) ware made. The experimental data for the 165 MW LP steam turbine obtained at the Institute for Turbomachinery, Hanover (Schmidt, Riess et al., 1995), ware used to check the numerical results. The design flow conditions at the turbine inlet are: $t_{in} = 100.21°C$, $p_{in} = 0.735bar$. The static pressure at the outlet is: $p_{out} = 0.05bar$. The calculations ware successfully performed for operating range $0.2\dot{m}_0 < \dot{m} < 1.0\dot{m}_0$ at constant inlet temperature. The loads with flow separation in the outlet diffuser and operation with power consumption of the turbine last stage ware also handled. More details about steam turbine flow calculations are published in the paper by Petrovic and Riess (1997). In the present analysis, Fig. 19 and Fig. 20 show the expansion process in the turbine and the stream function distribution for nominal and one part load. A portion of experimental results for this turbine is presented in Fig. 4

CONCLUSIONS

The method for through-flow calculation in axial flow turbines based on finite element procedure is presented herein. The applied models for loss coefficient prediction, radial loss distribution, spanwise mixing and deviation show good results. Validation of the method and computer program was done by the comparison of numerical results and experimental data for 4-stage experimental air turbine. The turbine overall performance was well predicted in the wide range of load. The Mass flow rate, at which value of pressure rate $\Pi \Rightarrow 1$, and the operating conditions at which the turbine starts to work with energy consumption are determined. Flow separation and reversal behind the rotor blade row, that had been detected experimentally at low load, were confirmed numerically. The agreement between predicted size of reverse flow region and experimental data is good. The method may be applied for flow calculation in both gas and steam turbines.

REFERENCES

Adkins, G.G. and Smith, L.H., 1981: "Spanwise Mixing in Axial Flow Turbomachines", ASME Paper No. 81-GT-57.

Ainley, D.G. and Mathieson,G.C.R., 1957: "A Method of Performance Estimation for Axial-Flow Turbine", ARC RM 2974

Baehr, H. D. and Diedrichsen, C., 1988: "Berechnungsgleichungen für Enthalpie und Entropie der Komponenten von Luft und Verbrenungsgasen", BWK, Vol. 40, pp. 30-33.

Bosman, C.and Marsh, H., 1974: "An Improved Method for Calculation the Flow in Turbo-Machines, including a Consistent Loss Model", J. Mech. Eng. Sci., Vol. 16, No. 1, pp. 25-31

Denton, J.D., 1978: "Throughflow Calculation for Axial Flow Turbines" Trans. of the ASME, J. of Eng. for Power, Vol. 100, pp. 212-218

Engeln-M"ullges, G., Reutter, F., 1988:, "Formelsammlung zur numerischen Mathematik mit Standard FORTRAN Programmen", BI-Wiss.-Verlag

Gallimore, S.J., 1986: "Spanwise Mixing in Multistage Axial Flow Compressors: Part II - Throughflow Calculations Including Mixing", Trans. of the ASME, J. of Turbomachinery, Vol. 108, pp. 10-16.

Groschup, G., 1977: "Strömungstechnische Untersuchung einer Turbinenstufe im Vergleich zum Verhalten der ebenen Gitter ihrer Beschaufelung", Diss. Univ. Hanover

Hirsch, Ch., Warzee, G., 1976: "A Finite Element Method for Through-Flow Calculations in Turbomachines", ASME Paper No. 76-FE-12

Hirsch, Ch. and Deconinck, H., 1985: "Through Flow Models for Turbomachines: Stream Surface and Passage Averaged

Representations", in: "Thermodynamics and Fluid Mechanics of Turbomachinery", Vol. I, ed. by Ucer, A.S., Stow, P., Hirsch, Ch., Martin Nijhoff Publishers, Dorderecht

Lewis,K.L., 1994: "Spanwise Transport in Axial-Flow Turbines", Part I and Part II, Trans. of the ASME, J. of Turbomachinery, Vol. 116, pp. 119-193

Petrovic, M. and Riess, W., 1997: "Off-Design Flow Analysis of LP Steam Turbines" to be published at 2nd European Conference "Turbomachinery - Fluid Dynamics and Thermodynamics", Antwerp, Belgium

Petrovic, M. and Riess, W., 1995: "Through-Flow Calculation in Axial Flow Turbines at Part Load and Low Load. 1st European Conference "Turbomachinery - Fluid Dynamic and Thermodynamic Aspects", Erlangen

Petrovic, M., 1995.: "Berechnung der Meridianströmung in mehrstufigen Axialturbinen bei Nenn- und Teillastbetrieb", Diss. Univ. Hanover, also: VDI Fortschrittberichte, Reiche 7, Nr. 280

Riess, W., Evers, B., 1985: "Die Str"omung in mehrstufigen Turbinen mit langen Schaufeln bei Schwachlast- und Leerlaufbetriieb", VGB Kraftwerkstechnik, Vol. 65, pp. 1020-1026

Saul, A.-H., 1988: "Eine Fundamentalgleichung für den fluiden Zustandsbereich von Wasser bis zu Drücken von 25000MPa und Temperaturen von 1273 K", VDI Fortschrittberichte, Reiche 3, Nr. 149, VDI Verlag.

Schmidt, D. and Riess, W. et al., 1995.: "Flow Studies on CHPP Turbines in Heating and Low-Load Operation", VGB Kraftwerkstechnik, 75(9) (also Germen issue)

Shcheglyaev, A. V., 1976: "Steam turbines", Energia, Moscow, (in Russian)

Smith, L.H., 1966: "The Radial-Equilibrium Equation of Turbomachinery", Trans. of the ASME, J. of Eng. for Power, Vol. 88, pp. 1-12.

Traupel, W., 1988: "Thermische Turbomaschinen", Vol. I, Springer-Verlag, Berlin

Wu, C. H., 1952: "A General Theory of Three-Dimensional Flow in Subsonic und Supersonic Turbomachines of Axial-, Radial- and Mixed-flow Types", NACA TN 2604, Washington

Zehner, P., 1980: "Calculation of Four-Quadrant Characteristics of Turbines", ASME Paper No. 80-GT-2.